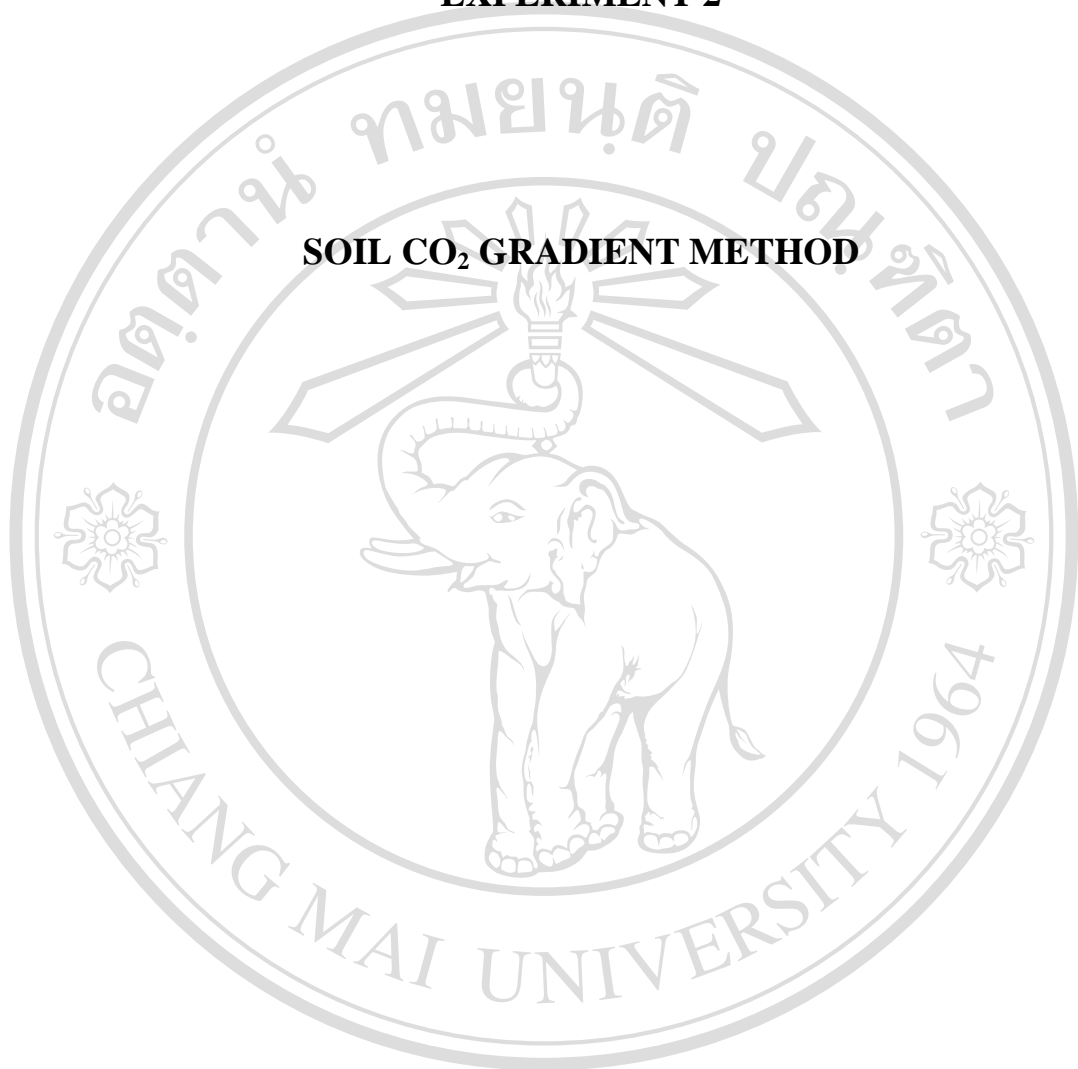


EXPERIMENT 2

SOIL CO₂ GRADIENT METHOD



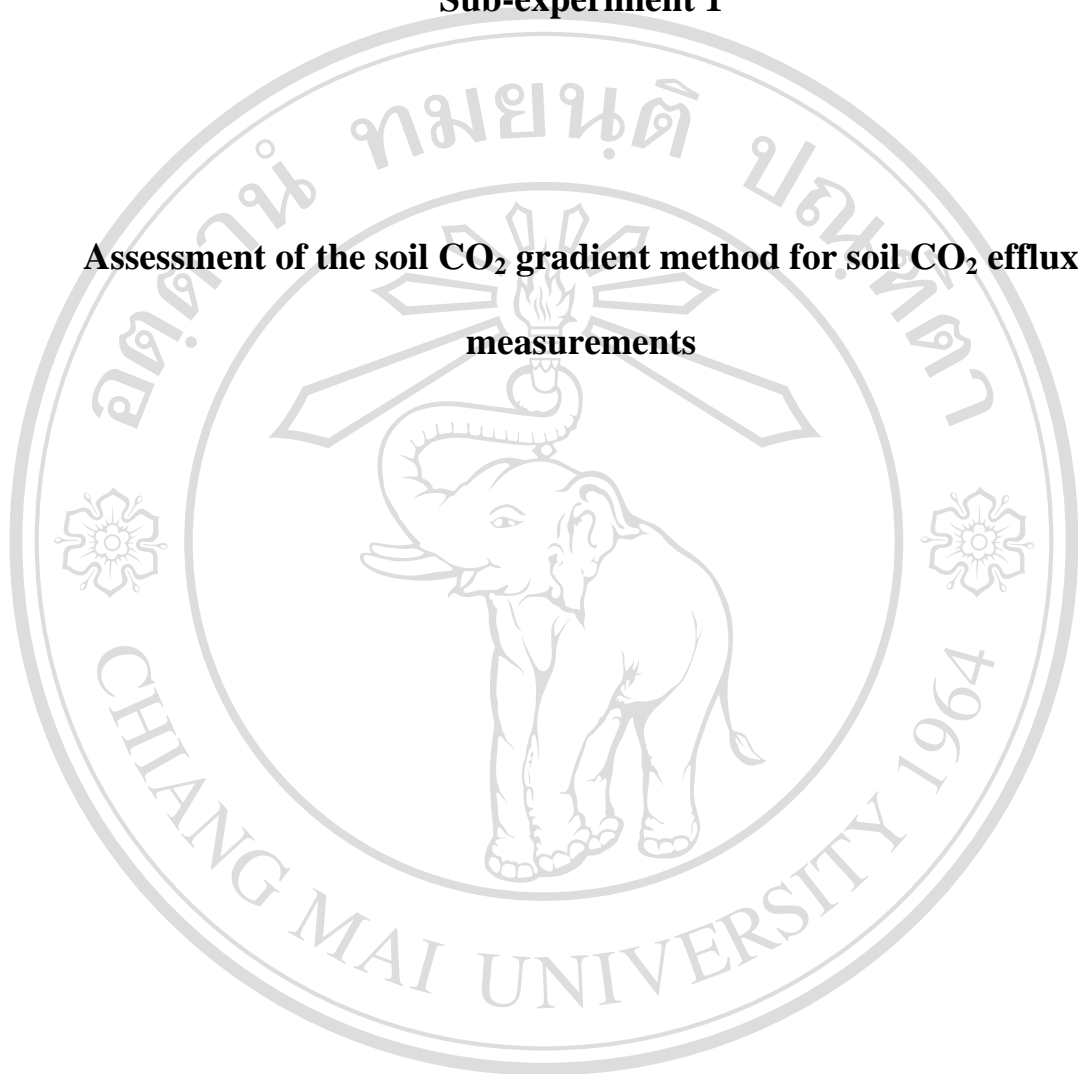
ลิขสิทธิ์มหาวิทยาลัยเชียงใหม่

Copyright© by Chiang Mai University

All rights reserved

Sub-experiment 1

**Assessment of the soil CO₂ gradient method for soil CO₂ efflux
measurements**



ลิขสิทธิ์มหาวิทยาลัยเชียงใหม่

Copyright© by Chiang Mai University

All rights reserved

INTRODUCTION

Concerns over global climate change have generated an interest in quantifying the role of agricultural soils as sources/sinks of atmospheric CO₂. This incentive has spurred research in evaluating soil carbon budgets and in elucidating the factors influencing soil carbon storage in agricultural ecosystems (Lal *et al.*, 1995; Lokupitiya and Paustian, 2006; Van Oost *et al.*, 2007). Soil CO₂ efflux is a combination of autotrophic root respiration and heterotrophic microbial respiration from the rhizosphere and bulk soil (Fang and Moncrieff, 1999). It is a major component of the terrestrial carbon cycle (Davidson *et al.*, 1999; Falk *et al.*, 2005; Stolbovoi, 2003), which can constitute up to approximately three-quarters of the total ecosystem respiration (Law *et al.*, 2001a). Soil CO₂ released to the atmosphere could potentially contribute to a positive feedback between increasing temperature and enhanced soil CO₂ efflux, ultimately accelerating global warming (Rodeghiero and Cescatti, 2005). To improve the robustness of carbon budget of terrestrial ecosystems, it is important to reduce uncertainties associated with the measurements of soil CO₂ efflux.

At present, soil CO₂ vertical gradient measurement method has become popular because it allows to continuously and automatically measure soil CO₂ flux at different temporal scales with a small disturbance to the natural soil structure a short time after installing the sensors (e.g. DeSutter *et al.*, 2008; Hirano *et al.*, 2003; Hirsch *et al.*, 2004; Jassal *et al.*, 2004; Jassal *et al.*, 2005; Myklebust *et al.*, 2008; Pumpanen *et al.*, 2008; Riveros-Iregui *et al.*, 2008; Tang *et al.*, 2003; Turcu *et al.*, 2005; Vargas

and Allen, 2008a; Vargas and Allen, 2008b; Vargas and Allen, 2008c) and is useful for comparison with other methods for ecosystem carbon exchanges such as the eddy-covariance method (Baldocchi *et al.*, 2006; Myklebust *et al.*, 2008). The soil CO₂ gradient method uses Fick's first law to calculate soil CO₂ efflux, relying on both measurements of soil CO₂ profile and on the CO₂ diffusion coefficient in the soil (D_s) (Davidson and Trumbore, 1995). Determining the latter with confidence is a challenge. Modeling as an approach can potentially be used to determine D_s . This is possible if some important soil properties (i.e., total soil porosity and air-filled porosity) are known. However, it is in practice difficult to accurately estimate D_s with either models or experimentally, and this limitation constitutes one of the main sources of error associated with the gradient method (Hutchinson and Livingston, 2002; Liang *et al.*, 2004).

When considering gas diffusion coefficients in soil, a relative gas diffusion coefficient (ξ), defined as the ratio of the gas diffusion coefficient in the soil to that in free air, is usually used. The highly dynamic nature of soil water content in the field may generate a non-uniform profile of air-filled porosity with depth. Therefore, the estimation of D_s from an average air-filled porosity is fraught with uncertainties and thus inadequate. Once detailed information on soil water content profile is obtained using the numerical model Hydrus-2D (Simunek *et al.*, 1999), Turcu *et al.* (2005) suggested determining the air-filled porosity for each discrete soil layer, and then applying a harmonic average to determine D_s for the considered whole soil profile in order to increase the reliability of the gradient method. D_s can be estimated as

$$D_s = \frac{\sum_{k=1}^n \Delta z_k}{\sum_{k=1}^n \frac{\Delta z_k}{D_{sk}(SWC_k)}} , \quad (4.1)$$

where $D_{sk}(SWC_k)$ represents soil gas diffusion coefficient for the discrete layer k with thickness Δz_k , and soil water content SWC_k , and n is the number of layers within the entire soil profile. However, further tests using the harmonically-averaged diffusion coefficients in field conditions are required.

The soil CO₂ gradient method's ability to accurately measure soil CO₂ efflux in a bare soil is assessed in this study. Non-steady-state chamber method is used as a reference to compare against the estimated CO₂ efflux using the soil CO₂ gradient method. Several models are used to calculate ξ and the harmonically-averaged diffusion coefficient is also tested.

It has been acknowledged that soil CO₂ efflux is highly correlated with environmental parameters, particularly soil temperature and soil moisture (e.g. Davidson *et al.*, 1998; Fang and Moncrieff, 1999; Jassal *et al.*, 2008; Jia *et al.*, 2006; Lloyd and Taylor, 1994). Whereas soil CO₂ efflux generally increases exponentially with temperature (e.g. Boone *et al.*, 1998; Davidson *et al.*, 1998; Epron *et al.*, 1999; Mielnick and Dugas, 2000), the relationship with soil moisture is more complex and depends on site specific soil parameters (Howard and Howard, 1993). To bolster confidence in the use of the soil gradient method, the functional relationships of soil CO₂ efflux to soil temperature and soil moisture are also investigated and discussed in this chapter.

MATERIAL AND METHODS

Site description

The experiment was conducted in a 4-ha rainfed peanut field at the Southwest Georgia Research and Education Center, Plains, Georgia, USA (32° 02' N, 84° 22' W, 156 m elevation) in 2006 (Figure 4.1). The site is nearly flat with a slope less than 2 degrees. Peanut variety Georgia Green (*Arachis hypogaea* L.) was planted on DOY 136 with a single row planting pattern, with a row space of 0.91 m and in-row plant population of 19 seed m⁻¹. They were harvested on DOY 282. The top 10 cm of soil is classified as Greenville sandy clay loam, composed of 56% of sand, 14% of silt, and 30% of clay, with a bulk density of 1.22 g cm⁻³ and with 0.04% of C and 0.56% of N. Soil texture and chemical composition were analyzed at the Soil, Plant, and Water Analysis Laboratory of the University of Georgia. A 3 m x 3 m sampling plot (bare soil) was established at the site on DOY 151, 2006. Any emerging crop in the plot was removed at the time of installation and the plot was kept free from any vegetation by weekly manual removal.



Figure 4.1 Photo of the study site in rainfed peanut at the Southwest Georgia Research and Education Center, Plains, Georgia, USA.

Soil CO₂ gradient method

Field measurements

Two CO₂ probes (GMP343, Vaisala Corp., Vantaa, Finland), based on the advanced CARBOCAP[®] Single-Beam Dual Wavelength non-dispersive infra-red (NDIR) technique, were deployed for *in situ* measurements of CO₂ concentration.

The probe is a cylinder of 194 mm in length and 55 mm in diameter and covered with a filter made of sintered PTFE (polytetrafluoroethylene) enabling gas exchange between the soil and the probe and protecting the probe from water. Over the PTFE filter, there is a protective cap made of 2-mm-thick POM (polyoxymethylene) and

having a diffusion slot of 1 mm in width and 50 mm in length where the gas enters the probe headspace through the PTFE filter. The sensor's CO₂ concentration measurement range is 0 to 5000 $\mu\text{mol mol}^{-1}$ with an accuracy of $\pm 2\%$ of reading. Each CO₂ probe consumes less than 1 W. The low power consumption minimizes the heating of soil; thus, an alteration of microclimate around the sensors can be avoided. The probes were installed horizontally with the diffusion slot downward at the depths of 0.02 and 0.12 m at the center of the sampling plot. These two depths were chosen to remain the probe readings within the dynamic range (0 to 5000 $\mu\text{mol mol}^{-1}$). Custom-built soil thermocouples were also installed at depths of 0.02, 0.05, 0.12, and 0.30 m and soil moisture sensors (CS615, Campbell Scientific, Logan, UT, USA) at 0.02 and 0.12 m. The latter were co-located with the soil CO₂ concentration probes to simultaneously measure soil temperature and moisture (Figure 4.2). Half-hourly averages of soil CO₂ concentration, soil temperature, and soil moisture profile measurements were recorded with a data logger (CR1000, Campbell Scientific, Logan, UT). The system was installed on DOY 189, 2006 and started to collect data immediately after the installation. Regarding the size of the probes one has to be aware that the soil is disturbed at the beginning. However, the disturbance is reduced sometime after installation of the probes (Tang *et al.*, 2005b; Tang *et al.*, 2003). To avoid the potential impact of soil disturbance on the soil CO₂ measurements, the data after DOY 264, 2006 when the soil environment of the probe had time to settle were used for the analysis in this study.

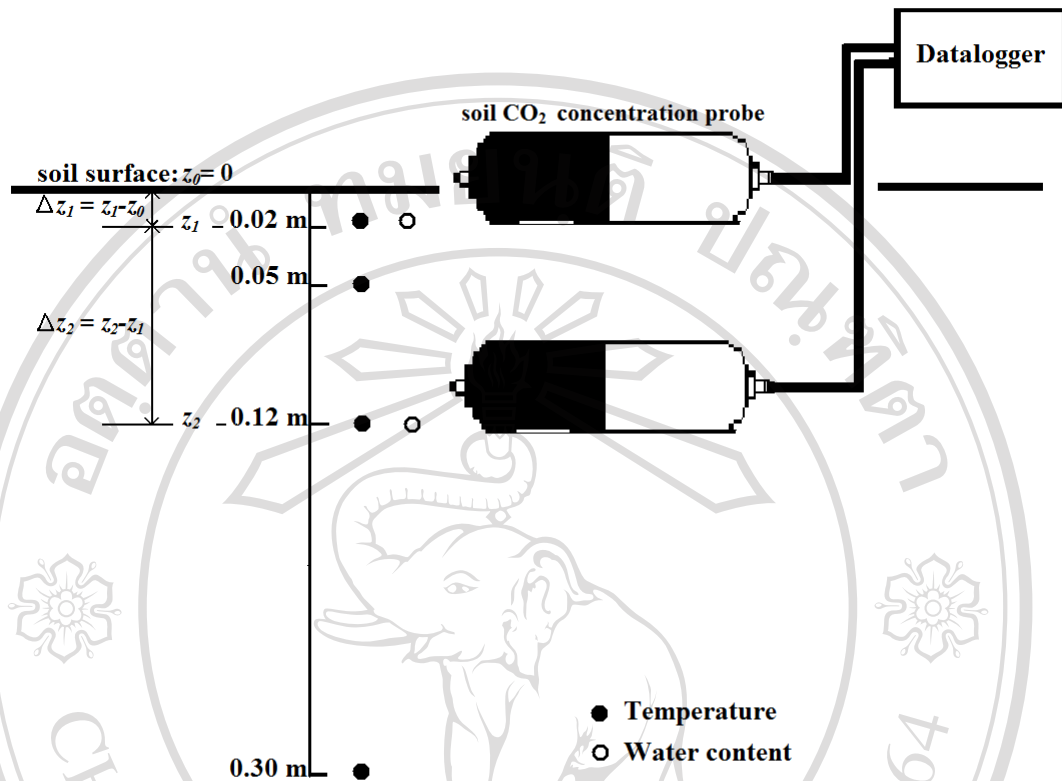


Figure 4.2 A schematic of the system for measuring soil CO₂ concentration, soil temperature and soil water content profiles.

Soil CO₂ efflux calculation

Measurements using the CO₂ sensors must be corrected for variations in temperature and pressure. This step was done by the manufacturer and subsequently used in the calculation of the soil surface CO₂ efflux. The soil CO₂ efflux (F_s , $\mu\text{mol m}^{-2} \text{s}^{-1}$) caused by diffusion is determined using Fick's first law:

$$F_s = -D_s \frac{\partial C(z)}{\partial z}, \quad (4.2)$$

where D_s is the CO₂ diffusion coefficient in the soil (m² s⁻¹) and C is the CO₂ concentration at a depth z (m) in the soil. The negative sign indicates that the efflux is in the reverse direction of the concentration gradient. D_s can be estimated as

$$D_s = \xi D_a, \quad (4.3)$$

where ξ is the relative gas diffusion coefficient or the gas tortuosity factor (Jury *et al.*, 1991), and D_a is the CO₂ diffusion coefficient in free air. The variation of D_a with temperature and pressure is given by

$$D_a = D_{a0} \left(\frac{T}{T_0} \right)^{1.75} \left(\frac{P}{P_0} \right), \quad (4.4)$$

where T is the temperature (K), P is the air pressure (Pa), and D_{a0} is a reference value of D_a at T_0 (20 °C or 293.15 K) and P_0 (1.013 x 10⁵ Pa), given as 1.47 x 10⁻⁵ m² s⁻¹ (Jones, 1992).

There are several empirical models used to determine ξ (Moldrup *et al.*, 2004; Sallam, 1984). In this study, six different existing models used to calculate ξ were compared:

$$\xi = 0.66(\phi - SWC) \quad (\text{Penman, 1940}), \quad (4.5)$$

$$\xi = (\phi - SWC)^{1.5} \quad (\text{Marshall, 1959}), \quad (4.6)$$

$$\xi = \frac{(\phi - SWC)^{10/3}}{\phi^2} \quad (\text{Millington and Quirk, 1961}), \quad (4.7)$$

$$\xi = 0.66(\phi - SWC) \left(\frac{\phi - SWC}{\phi} \right)^{\frac{12-m}{3}} \quad (\text{Moldrup et al., 1997}), \quad (4.8)$$

$$\xi = \phi^2 \left(\frac{\phi - SWC}{\phi} \right)^{\beta S} \quad (\text{Moldrup } et al., 1999), \quad (4.9)$$

$$\xi = \frac{(\phi - SWC)^{2.5}}{\phi} \quad (\text{Moldrup } et al., 2000), \quad (4.10)$$

where SWC is the volumetric soil water content, $\phi = \rho_b / \rho_m$ is the porosity (where ρ_b is the bulk density (g cm^{-3}) and ρ_m is the particle density of mineral soil with a typical value of 2.65 g cm^{-3}), S is the percentage of mineral soil with particle size $> 2 \mu\text{m}$ (0.44 at our site), and m and β are constants, equal to 3 and 2.9 respectively.

The vertical distribution of soil water content in the soil profile is generally considered as non-uniform. Based on Equation 4.1, D_s can be estimated as:

$$D_s = \frac{\Delta z_1 + \Delta z_2}{\frac{\Delta z_1}{D_{sz_1}(SWC_{z_1})} + \frac{\Delta z_2}{D_{sz_2}(SWC_{z_2})}}, \quad (4.11)$$

where the subscript denotes depth (Figure 4.2).

Soil CO₂ efflux measurements by Li-8100 non-steady state chamber system

To validate the soil CO₂ gradient method, results from this method were compared with soil CO₂ efflux measured with a soil respiration chamber. Five soil collars, each with a height of 4.4 cm and a diameter of 11 cm, were inserted into the soil in the vicinity of the soil CO₂ gradient system in the sampling plot on DOY 256. Periodic measurements of soil CO₂ efflux were made using a Li-8100 soil CO₂ flux system (Licor, Lincoln, NE) equipped with a 10 cm survey chamber with an accuracy of $\pm 1.5\%$ of the reading (Figure 4.3). The chamber was put on a PVC collar for a 2-

min duration following a 30-s dead band (the time until steady chamber mixing is established) to measure soil CO₂ efflux and then moved to the next collar. In this study, five collars were measured within a 30-min period to complete a full measurement cycle. Soil CO₂ efflux was estimated by calculating the initial slope of a fitted exponential curve at the ambient CO₂ concentration. This was done to minimize the effect resulting from the altered CO₂ concentration gradient across the soil surface after the chamber closed. The soil CO₂ gradient method is compared with the soil respiration chamber method when the latter was also applied at the sampling plot on DOY 265, 269, 271, 272, 273, 277, 278, and 282 (harvest day) in 2006. The soil chamber measurements were taken during 8:30 h to 19:00 h.



Figure 4.3 The photo of the comparison of the soil CO₂ gradient method and the Li-8100 soil chamber in a 3x3 m sampling plot.

Environmental measurements

An automatic weather station (ET106, Campbell Scientific, Logan, UT) was installed at 1.5 m above the ground surface at the study site for measuring important environmental parameters such as air temperature, relative humidity, wind speed and wind direction, solar radiation, and precipitation. The weather station sampled the data every two seconds and output 30-min averages. Moreover, net radiation was measured using a net radiometer (Model NR-LITE, Kipp and Zonen USA Inc., Bohemia, NY) mounted 1.8 m above the ground surface at a tower located 15 m northwest from the automatic weather station tower. The 30-min average data were recorded with data loggers (CR10X, Campbell Scientific, Logan, UT) and then transferred to a laptop computer. The maximum net radiation varied from 470 to 594 W m^{-2} . During the period of soil chamber measurements, the mean wind speed varied from 0.05 to 6.80 m s^{-1} , mean soil temperature at the depth of 0.05 m from 16 to 31 $^{\circ}\text{C}$, and mean air temperature from 10 to 31 $^{\circ}\text{C}$. Two rain events were recorded on DOY 267 (9.7 mm) and DOY 268 (2.5 mm) during the period of the comparison, but no precipitation event was observed on the dates that soil chamber measurements were performed.

Data analysis

In the present analysis, the 30-min average soil CO_2 efflux from the soil gradient method were compared with the mean of soil chamber measurements across all five collars in the same 30-min period. The coefficient of variation was used to represent the spatial variation in soil CO_2 efflux measured using the Li-8100 chamber. Linear and non-linear regression analyses were used to examine the relationship

between soil CO₂ efflux (obtained using the gradient method on days that the soil chamber measurements were performed) and environmental variables.

In order to confirm the ability of the gradient method, the functional relationships of soil CO₂ efflux to soil temperature and soil moisture were examined in the light of previous studies. The relationship between soil CO₂ efflux and soil temperature (T_s) was represented by (e.g. Boone *et al.*, 1998; Davidson *et al.*, 1998; Epron *et al.*, 1999; Mielnick and Dugas, 2000):

$$F_s(T_s) = ae^{bT_s}, \quad (4.12)$$

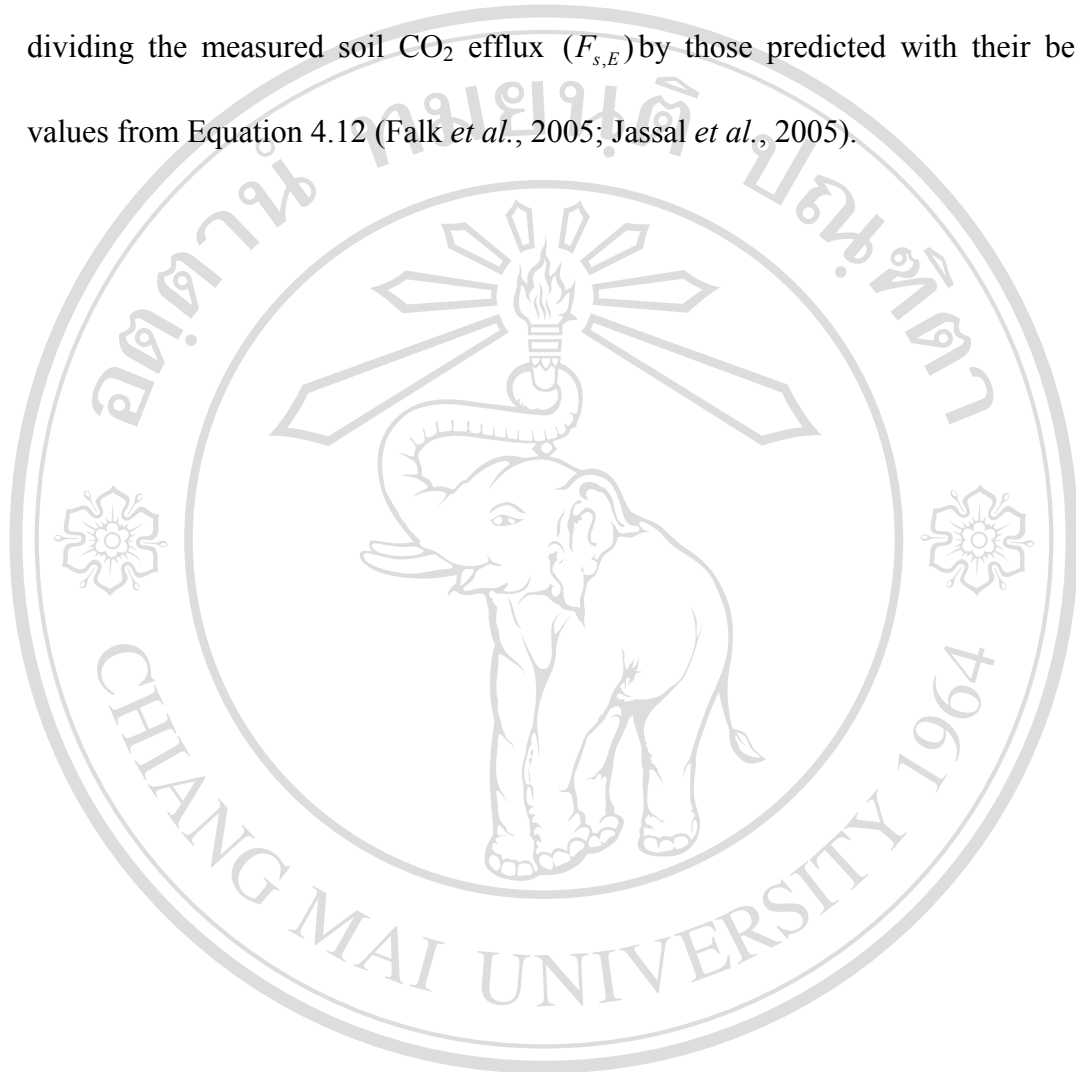
where a and b are coefficients estimated by the non-linear regression. a denotes the reference soil CO₂ efflux at 0 °C and b provides an estimate of the Q_{10} coefficient, representing the degree of the dependence of soil CO₂ efflux on soil temperature. The latter coefficient was calculated according to the following equation:

$$Q_{10} = e^{10b}, \quad (4.13)$$

To isolate the effect of soil water content variation on soil CO₂ efflux F_s , the temperature-normalized efflux plotted against the soil water content were fitted with a linear function (Davidson *et al.*, 1998; Epron *et al.*, 1999):

$$F_{s,E} / F_s(T_s) = c + dSWC, \quad (4.14)$$

where c and d are coefficients estimated by the linear regression and SWC is the volumetric soil water content. The temperature-normalized efflux was obtained by dividing the measured soil CO_2 efflux ($F_{s,E}$) by those predicted with their best-fit values from Equation 4.12 (Falk *et al.*, 2005; Jassal *et al.*, 2005).



ลิขสิทธิ์มหาวิทยาลัยเชียงใหม่
Copyright© by Chiang Mai University
All rights reserved

RESULTS AND DISCUSSION

Soil CO₂ efflux

An *in situ* comparison of soil CO₂ efflux using both methods in the sampling plot was conducted on the above-stated eight occasions throughout the experimental period. Fick's first law was used to determine the soil CO₂ efflux using the CO₂ concentration at two depths ($z_1=0.02$ m and $z_2= 0.12$ m) and the calculated soil diffusion coefficient ξ . Among the models used to calculate ξ , the models proposed by Penman (1940) yielded the highest soil CO₂ efflux values (Table 4.1). The mean of soil CO₂ efflux values across all five collars within 30-min period obtained using the Li-8100 soil chamber in the sampling plot ranged from 0.53 to 1.52 $\mu\text{mol m}^{-2} \text{s}^{-1}$, with an average of $0.91 \pm 0.24 \mu\text{mol m}^{-2} \text{s}^{-1}$ over the entire campaign. This mean value was in the range of soil CO₂ efflux obtained for bare soil in agricultural fields in China (0.20-1.58 $\mu\text{mol m}^{-2} \text{s}^{-1}$; Ding *et al.*, 2007) and Japan (0.57-1.94 $\mu\text{mol m}^{-2} \text{s}^{-1}$; Nakadai *et al.*, 2002).

Table 4.1 Summary of maximum, minimum, and average of the half-hourly soil CO₂ efflux determined with the gradient method and the mean of soil CO₂ efflux measurements across all five collars within 30-min period obtained using the Li-8100 soil chamber on DOY 265, 269, 271, 272, 273, 277, 278, and 282 in 2006. Statistical parameters describe the linear regression relationships between soil CO₂ efflux from Li-8100 chamber and estimated CO₂ efflux by the gradient method with different gas diffusivity model [Equation 4.5 – 4.10].

Gradient Method	Estimated Soil CO ₂ Flux ($\mu\text{mol m}^{-2} \text{s}^{-1}$)			Parameter			
	Gas Diffusivity Model	Maximum	Minimum	Average	Slope	Intercept	R ^{2†}
Penman (1940)		4.22	1.08	2.54	2.73±0.22	0.07±0.20	0.61**
Marshall (1959)		4.04	1.06	2.44	2.59±0.20	0.09±0.19	0.62**
Millington and Quirk (1961)		2.56	0.74	1.56	1.58±0.12	0.13±0.11	0.66**
Moldrup <i>et al.</i> (1997)		1.69	0.51	1.03	1.03±0.07	0.10±0.07	0.67**
Moldrup <i>et al.</i> (1999)		2.98	0.83	1.81	1.88±0.13	0.11±0.13	0.64**
Moldrup <i>et al.</i> (2000)		2.53	0.68	1.53	1.61±0.12	0.08±0.11	0.63**
Soil Chamber Method		1.52	0.53	0.91			

†Coefficient of determination

± Standard error

**Significant at $P \leq 0.01$

A linear regression analysis was applied to investigate the relationship between half-hourly mean soil CO₂ efflux values of the soil gradient method calculated using different ξ models and the mean of the five collars of Li-8100 chamber measurements during simultaneous 30 minutes. The estimated soil CO₂ efflux results from the soil gradient method differed from the Li-8100 chamber method by 173, 159, 58, 3, 88, and 61% for the Penman (1940), Marshall (1959), Millington and Quirk (1961), Moldrup *et al.* (1997), Moldrup *et al.* (1999), and Moldrup *et al.* (2000) models, respectively (Table 4.1). Indeed, the differences between soil CO₂ efflux obtained using the soil gradient method with different empirical models used to determine ξ and soil chamber method have been observed in forests (Jassal *et al.*, 2005; Liang *et al.*, 2004), savanna ecosystems (Tang *et al.*, 2003), grasslands (Myklebust *et al.*, 2008), and greenhouses (Turcu *et al.*, 2005), but not so much in agricultural ecosystems. It is possible that the uncertainty in the soil CO₂ efflux calculation is attributed mostly to the model used to estimate ξ , as reported by Jassal *et al.* (2005), who found that Penman (1940) and Marshall (1959) models overestimated diffusivities while the Millington and Quirk (1961) and Moldrup *et al.* (1999) models underestimated them at very low air-filled porosity. Iiyama and Hasegawa (2005) also showed that the Millington and Quirk (1961) model underestimated measured diffusivity for low air-filled porosity and overestimated them for high air-filled porosity. Sallam *et al.* (1984) and Jin and Jury (1996) pointed out the same kind of erroneous estimation when the Millington and Quirk (1961) model was used.

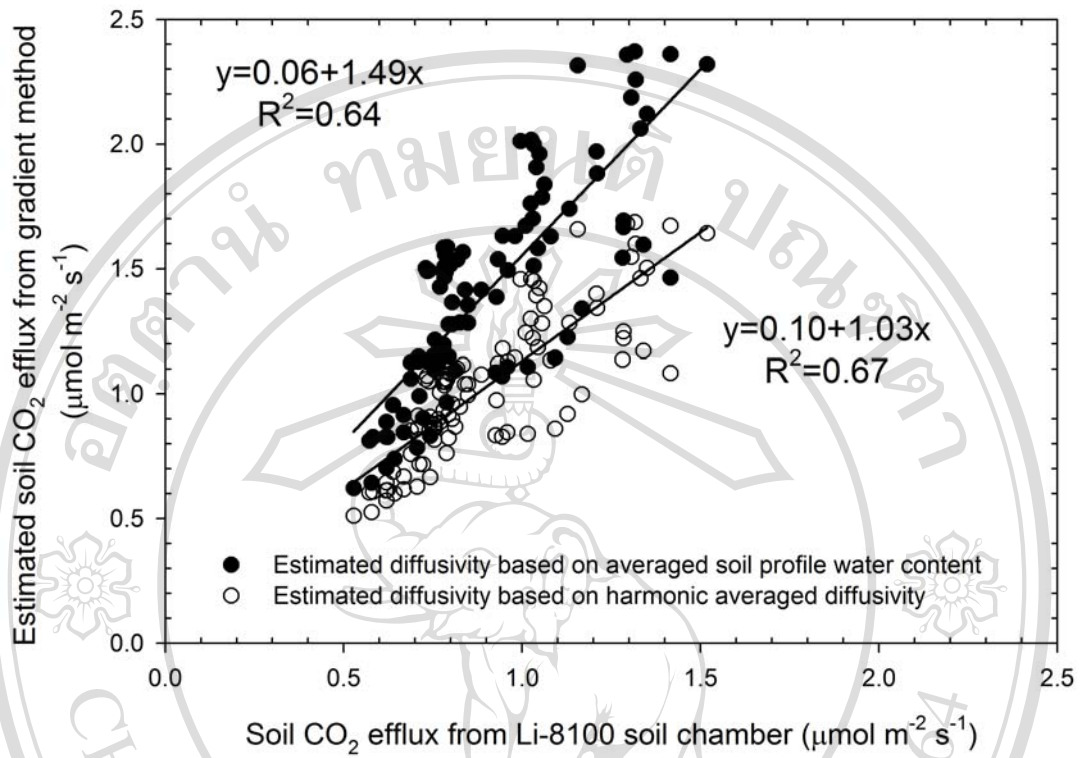


Figure 4.4 Linear relationship between the half-hourly mean estimated CO₂ efflux by the gradient method and the mean of soil CO₂ efflux measurements across five collars obtained by Li-8100 chamber during the same 30-min periods. Soil gas diffusivity in the gradient method was estimated with two approaches based on averaged soil profile water content and based on harmonic averaged diffusivity. The two straight

lines are fitted regression lines.

Among the models used to obtain ξ , the Moldrup *et al.* (1997) model yielded soil CO₂ efflux values closest to the results of the soil chamber method and gives on average 3% ($R^2 = 0.67$) greater efflux than the soil chamber method (Table 4.1). Moldrup *et al.* (1997) model combined the Penman (1940) and Millington and Quirk (1961) models together to develop a general (independent of soil type) model and gave an improved description of the previous models (Moldrup *et al.*, 1997).

In field conditions, spatial variations in textural properties in a soil profile and non-uniform vertical distribution of soil water content need to be considered. The variation especially in soil water content is of particular interest since it affects the calculations of an effective gas diffusion coefficient in a given soil layer. For a layered non-uniform soil profile with transport perpendicular to layering, the calculations of the effective diffusion coefficient based on the weighted harmonic average of individual diffusivity of each layer are required. Turcu *et al.* (2005) used solid-state CO₂ sensors to measure soil CO₂ concentration in greenhouse soil columns in transient-state soil water content and temperature conditions. They found that the soil CO₂ efflux determined with the gradient method was about three times higher than the CO₂ flux measured with the soil chamber when diffusivities were obtained using the average soil profile water content. However, there was a better agreement with the soil chamber when the weighted harmonically-averaged diffusion coefficients were used. Similarly, the present study find that the estimated soil CO₂ efflux using the gradient method with the Moldrup *et al.* (1997) model and the weighted harmonically-averaged diffusion coefficients show a closer agreement with the soil chamber data than that with the same ξ model but the profile-averaged soil water content (Figure 4.4). With a slope of 1.03, an intercept of 0.10, and $R^2 = 0.67$,

the estimated soil CO₂ efflux is only 3% on average greater than that from the soil chamber method (Figure 4.4). The 3% difference in the measurements could be due to the fact that the soil gradient method overestimates efflux in the late afternoon (Figure 4.5a). The efflux from the soil gradient method is calculated from soil CO₂ concentration gradient ($\Delta C/\Delta z$) between the layers of 0.02 and 0.12 m and is controlled by soil temperature. We investigated the soil temperature between those layers (0.05 m) and $\Delta C/\Delta z$ peaked in the afternoon (Fig. 4.5b, c). Thus, the soil CO₂ efflux from the gradient method does not show the depression in the afternoon. This leads to an overestimate of the efflux.

The coefficient of variation calculated for each set of CO₂ measurements across five collars in 30 minutes varied from 16 to 49%, and averaged 30% (data not shown). Given that the 3% difference between the gradient method (the stationary point measurements) and the soil chamber method (the five spatial measurements) was less than the 30% uncertainty due to spatial variation in soil efflux, measurements of soil CO₂ efflux obtained using the gradient method are statistically equivalent to those obtained using the soil chamber method.

The modest level of correlation ($R^2=0.67$) between results obtained by the gradient method and by the soil chamber method can be attributed to the following two reasons. First, the efflux from the chamber method is the efflux at the ground surface while the efflux from the gradient method is the vertical mean efflux below the surface (in this study, the CO₂ efflux was calculated between the layers of 0.02 and 0.12 m). It is difficult to perfectly estimate the soil CO₂ concentration gradient near the surface. To determine the soil CO₂ efflux at the surface, the measurements of soil CO₂ concentration at several depths are needed. Assuming that the soil CO₂

concentration linearly decreases with soil depth, the soil CO₂ efflux at the soil surface can be calculated at soil depth equal to zero (Tang *et al.*, 2005b; Vargas and Allen, 2008a). However, these assumptions become invalid when soil CO₂ is greater in shallow soils than in deeper soils, such as during a sudden precipitation event during a long dry summer, due to bidirectional concentration gradients and fluxes (Tang *et al.*, 2005b; Vargas and Allen, 2008a). In this study, the ability to measure soil CO₂ concentration at multiple depths was limited by the measurement range of the sensor. Nonetheless, the difference between surface CO₂ efflux values and those taken just beneath the surface as in this experiment are expected to be small (3%) as shown in previous studies (Liang *et al.*, 2004; Myklebust *et al.*, 2008; Tang *et al.*, 2003). Another apparent source of uncertainties lies in the spatial and temporal averages of both methods. The estimated soil CO₂ efflux from the gradient method was calculated using 30-min average output data. This method provides a longer continuous-measurement period at the expense of spatial averaged information. On the other hand, the soil CO₂ efflux from the soil chamber method was calculated using the average of the measurements across all five collars in the same 30-min period. The total measurement time used to calculate the soil CO₂ efflux is approximately 10 min for every measurement cycle (i.e. two-minute average for the soil chamber placed over each collar for five collars), providing a greater spatial distribution of measurements this time, at the expense of temporal resolution.

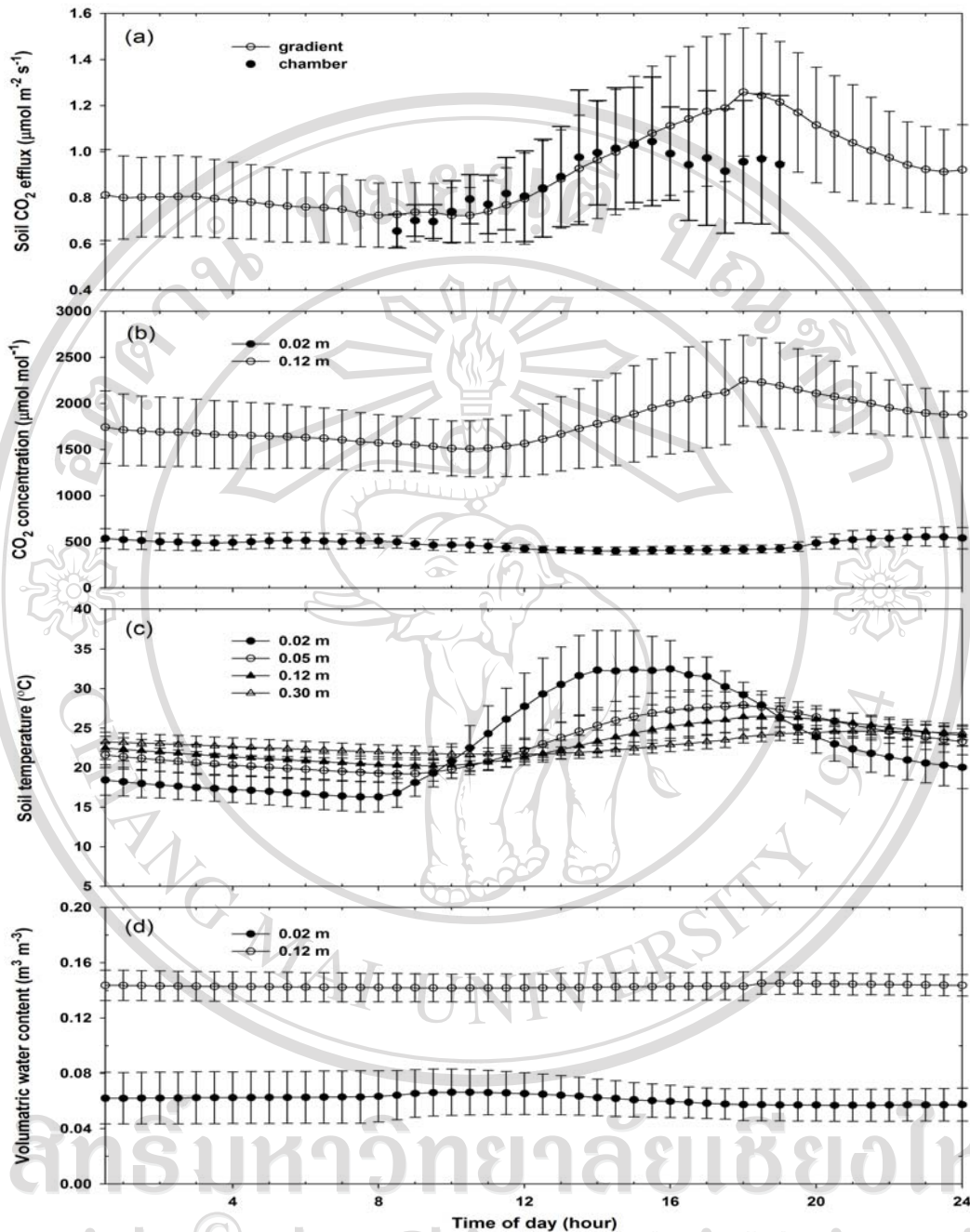


Figure 4.5 Mean diurnal variations and their standard deviation on DOY 265, 269, 271, 272, 273, 277, 278, and 282 in 2006. (a) Soil CO₂ efflux determined with the gradient method using the Moldrup *et al.* (1997) model to obtain ξ (closed circles) and the mean of soil CO₂ efflux measurements across all five collars within 30-min period obtained using the Li-8100 soil chamber (open circles); (b) soil CO₂ concentration at depths of 0.02 and 0.12 m; (c) soil temperature at depths of 0.02, 0.05, 0.12, and 0.30 m; (d) volumetric soil water content at depths of 0.02 and 0.12 m (ensemble average for each half-hour).

Diurnal variation of soil CO₂ profile in measurements

Figure 4.5 shows the mean diurnal variations of soil CO₂ efflux, soil CO₂ concentration, soil temperature, and volumetric soil water content, averaged over all days in which the soil chamber measurements were available. The diurnal variation of soil CO₂ concentration at the 0.12 m depth and soil CO₂ efflux from the soil CO₂ gradient method showed a similar temporal pattern (Figure 4.5a, b). They peaked at around 18:00 h, 2 to 4 h later than the peak of soil temperature at the 0.02 m depth (Figure 4.5a, b, and c). Unlike the CO₂ concentration at the 0.12 m depth and soil CO₂ efflux, the diurnal variation of CO₂ concentration at the 0.02 m depth showed differently. Between 14:00 to 16:00 h when soil temperature at the 0.02 m depth showed the highest value within a day, the CO₂ concentration at the 0.02 m depth had a minimum value (Figure 4.5b, c). It is clear that soil temperatures at deeper depths have delayed diurnal courses (Figure 4.5c). The temperature at 0.02 m peaked early while the temperature at 0.30 m peaked late. In addition, the amplitudes of soil temperature decreased with depth. Volumetric soil water content at the 0.02 and 0.12 m depth had no significant diurnal variation (Figure 4.5d).

The reason for decreased CO₂ concentration in the top soil layer (0.02 m depth) at high soil temperature has been discussed. Tang *et al.* (2003) attributed this result to the CO₂ production rate and diffusivity at that layer: CO₂ production rates are sensitive to soil temperature, but any additional increase in temperature may decrease the temperature sensitivity and CO₂ production rates (Kirschbaum, 1995; Lloyd and Taylor, 1994; Xu and Qi, 2001). Therefore, the CO₂ concentration at 0.02 m did not peak in the early afternoon probably due to the extremely high temperature in the top soil layer. Another reason for the decreased CO₂ concentration under high

temperature is the transport of CO₂. The high transport rate of CO₂ may prevent CO₂ from building-up in the top layer during early afternoon because CO₂ diffusivity increases with temperature (Tang *et al.*, 2003). In addition to soil biological and physical factors, the surface wind may also affect CO₂ concentration. This study found the highest surface wind speed occurred during the early afternoon (data not shown), corresponding to decrease CO₂ concentration at 0.02 m.

Soil CO₂ efflux and its correlation with soil temperature and soil moisture

An examination of Table 4.2 reveals that soil CO₂ efflux correlated exponentially with soil temperature, with the highest R² of 0.54 at the depth of 0.05 m (Figure 4.6). The coefficient Q_{10} increased with the depth of soil temperature probes, i.e. 1.24 (R²=0.27), 1.81 (R²=0.54), 2.23 (R²=0.53), and 3.03 (R²=0.28) for depth 0.02, 0.05, 0.12, and 0.30 m, respectively. Similar results have been reported by Hirano *et al.* (2003), Tang *et al.* (2003), Pavelka *et al.*(2007), Graf *et al.* (2008) (2008), and Peng *et al.* (2008). Pavelka *et al.* (2007) and Graf *et al.* (2008) suggesting that since the amplitude of soil temperature dynamics generally decreases with an increase in soil depth, the Q_{10} value derived from changes in soil respiration and soil temperature may increase with the depth of the soil temperature measuring point, which is consistent with our presented results (Figure 4.5c).

Table 4.2 Fit of equation $F_s(T_s) = ae^{bT_s}$ to access the relationship between the half-hourly soil CO₂ efflux determined with the gradient method using the Moldrup *et al.* (1997) model to obtain ξ and soil temperature and $F_{s,E} / F_s(T_s) = c + dSWC$ to access the relationship between the half-hourly temperature-normalized efflux and soil water content on DOY 265, 269, 271, 272, 273, 277, 278, and 282 in 2006.

Soil Temperature	Parameter			
Soil Depth (m)	a	b	Q_{10}	R ^{2†}
0.02	0.54±0.03	0.02±0.00	1.24	0.27**
0.05	0.23±0.02	0.06±0.00	1.81	0.54**
0.12	0.14±0.01	0.08±0.00	2.23	0.53**
0.30	0.07±0.02	0.11±0.01	3.03	0.28**
Soil Water Content	Parameter			R ^{2†}
Soil Depth (m)	c	d		
0.02	0.41±0.03	9.61±0.42		0.59**
0.12	-1.50±0.07	17.61±0.54		0.74**

†Coefficient of determination

± Standard error

**Significant at $P \leq 0.01$

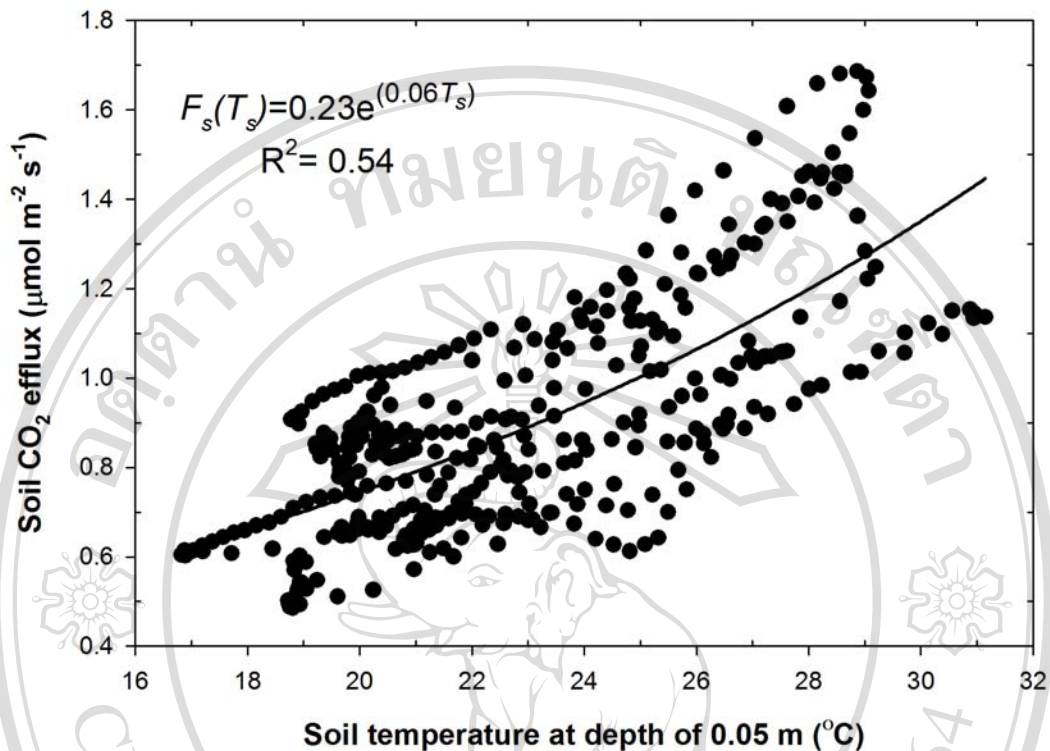


Figure 4.6 Relationship between the half-hourly estimated soil CO₂ efflux by the gradient method using the Moldrup *et al.* (1997) model to obtain ξ and soil temperature at 0.05 m depth on days DOY 265, 269, 271, 272, 273, 277, 278, and 282 in 2006. The non-linear regression curve was fitted with Equation 4.12.

Results indicate that diurnal variations of soil CO₂ efflux were usually out of phase with soil temperature at the 0.02 m depth (Figure 4.5a, c). Soil CO₂ efflux reached the peak values approximately between 17:30 and 18:00 h, 2 to 4 h later than soil temperature at 0.02 m depth. This resulted in significant counterclockwise hysteresis in the relationship between half-hourly soil CO₂ efflux and soil temperature at the 0.02 m depth, indicating an apparent differential response of soil CO₂ efflux to soil warming and to soil cooling (Figure 4.7a). Soil CO₂ efflux increased in response

to soil warming in the morning and decreased when soil temperature started to cool. On the other hand, soil temperature at the depths of 0.12 and 0.30 m peaked later than soil CO₂ efflux, resulting clockwise hysteresis (Figure 4.7c, d). Volumetric soil water content at 0.02 m and 0.12 m depths had no significant diurnal variation (Figure 4.5d) indicating that volumetric soil water content was not responsible for the hysteresis behavior. The diel hysteresis effects on soil CO₂ efflux, i.e. the sum of heterotrophic respiration (by decomposers) and autotrophic respiration (by roots and mycorrhizas), have been reported for different ecosystems (Gaumont-Guay *et al.*, 2006; Parkin and Kaspar, 2003; Riveros-Iregui *et al.*, 2008; Riveros-Iregui *et al.*, 2007; Tang *et al.*, 2005a; Vargas and Allen, 2008a; Vargas and Allen, 2008b; Vargas and Allen, 2008c). Riveros-Iregui *et al.* (2007) and Vargas and Allen (2008c) have proved that the diel hysteresis was explained by mechanisms, including the temperature-dependent component of soil CO₂ efflux and its dependence on photosynthetically active radiation (*PAR*). However, our study was conducted in bare soil without the presence of roots; therefore, it is assumed that soil CO₂ efflux is solely from heterotrophic respiration, implying that the effect of *PAR* on diel hysteresis is negligible in this study. There is no clear mechanistic explanation for this response yet, further study is

needed.

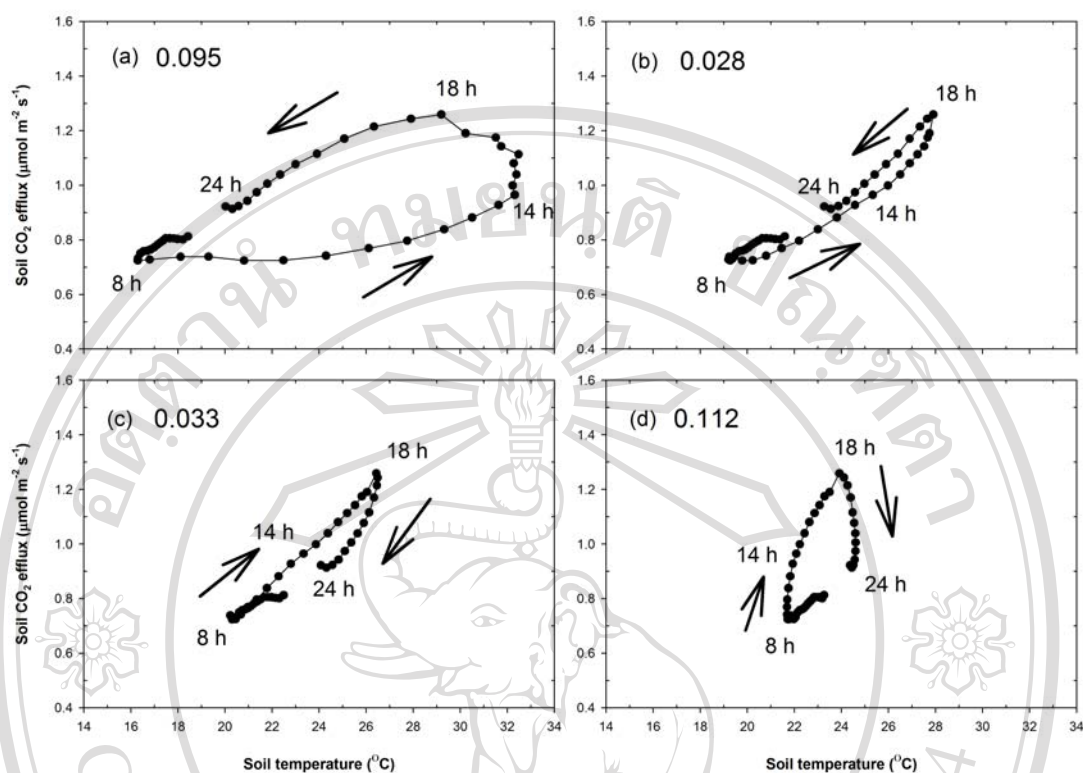


Figure 4.7 Relationship between soil CO₂ efflux determined with the gradient method using the Moldrup *et al.* (1997) model to obtain ξ and soil temperature at the depths of (a) 0.02, (b) 0.05, (c) 0.12, and (d) 0.30 m for measurements made on DOY 265, 269, 271, 272, 273, 277, 278, and 282 in 2006 (ensemble average for each half-hour). The arrows indicate the direction of the hysteresis effect. The numbers indicate the

mean absolute residual. Residual values calculated as the difference between measured soil CO₂ efflux and modeled (Equation 4.12) values were used to assess the magnitude of hysteresis.

The Q_{10} value (1.24) calculated based on soil temperature at the depth of 0.02 m is less than half of that estimated by soil temperature at the depth of 0.30 m (3.03). This result indicates that the choice of soil temperature measuring depth in analysis can influence the results. Therefore, it is a significant challenge to find a suitable depth for measuring soil temperature which can minimize the predicted errors of soil CO₂ efflux using temperature as independent variable. Pavelka *et al.* (2007) pointed out that the most suitable soil temperature measurement depth is the soil surface temperature because of the optimized regression coefficient between soil surface temperature and soil CO₂ efflux. In addition, Gaumont-Guay *et al.* (2006) suggested that the response curve of soil CO₂ efflux to soil temperature with the lowest hysteresis indicates the most appropriate temperature measurement depth. In this study, the temperature at the depth of 0.05 m yielded the highest correlation coefficient (Table 4.2) with the lowest hysteresis (Figure 4.7b). According to the results from this and previous (Gaumont-Guay *et al.*, 2006; Pavelka *et al.*, 2007) studies, this infer that the temperature at the depth of 0.05 m was the most appropriate to examine the measured relationship between soil CO₂ efflux and soil temperature.

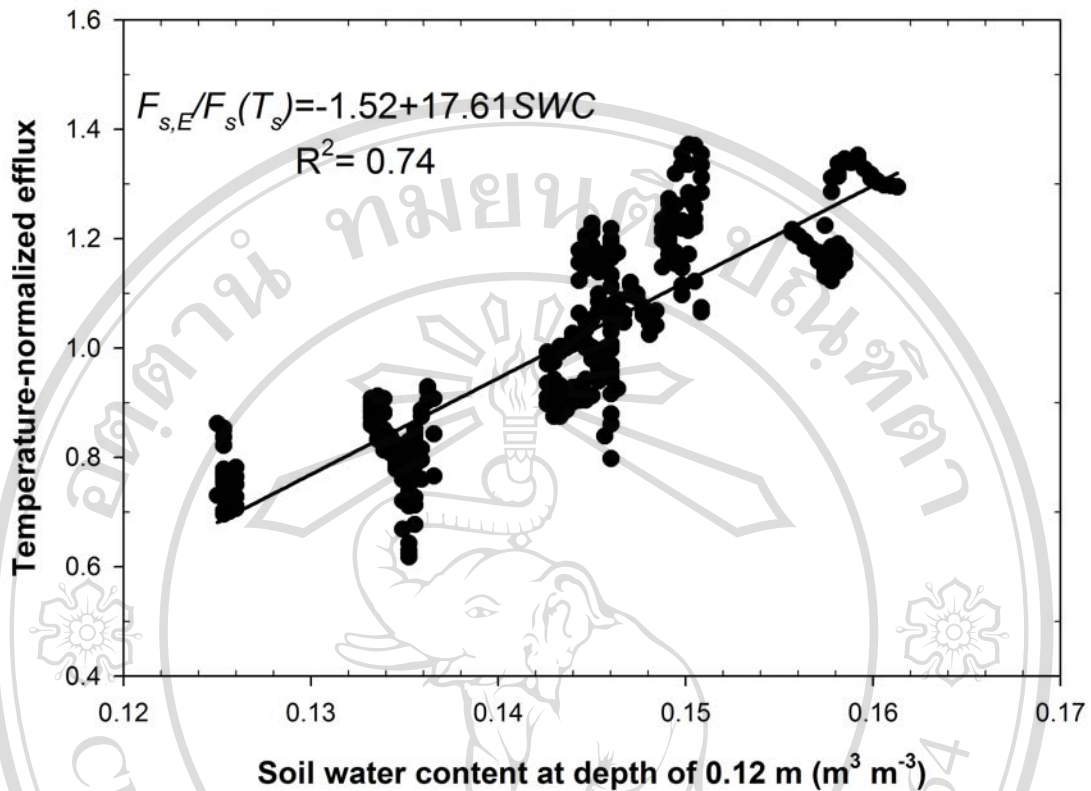


Figure 4.8 Relationship between the half-hourly temperature-normalized efflux and soil water content at 0.12 m depth on DOY 265, 269, 271, 272, 273, 277, 278, and 282 in 2006. The linear regression curved was fitted with Equation 4.14.

Since both soil moisture and soil temperature influence CO₂ efflux, it is often difficult to extirpate the degree to which each of these variables plays in soil respiration (Davidson *et al.*, 1998). To isolate the effect of soil water content variation on soil CO₂ efflux, the temperature-normalized efflux was used and their relationship with the soil water content was fitted with Equation 4.14. Soil water content at the depths of 0.02 and 0.12 m explained 59 and 74 % of the temperature-normalized efflux, respectively (Table 4.2). The influence of moisture content on soil CO₂ efflux is complex through its effect on respiratory activity of roots and microbes (Vargas and

Allen, 2008c) and gas transport through the soil (Fang and Moncrieff, 1999). Generally, soil CO₂ efflux increases as soil moisture increases, but soil moisture content can inhibit soil CO₂ efflux significantly at its low (dry soil) and high end (wet soil). The soil water content at 0.12 m was in a range of 0.125-0.161 m³ m⁻³ and there was no evidence for extremely dry and wet soils in this study. Thus, the relationship between soil CO₂ efflux and soil moisture was best described using a linear equation (Figure 4.8) (Davidson *et al.*, 1998; Epron *et al.*, 1999).

The functional relationships of soil CO₂ efflux to soil temperature and soil moisture and the existence of hysteresis between soil CO₂ efflux and soil temperature from this study are consistent with previous findings, confirming that the soil gradient method combined with weighted harmonic averaging for diffusion coefficients can reliably be used to measure soil CO₂ emissions.